

RSC Advances



This is an *Accepted Manuscript*, which has been through the Royal Society of Chemistry peer review process and has been accepted for publication.

Accepted Manuscripts are published online shortly after acceptance, before technical editing, formatting and proof reading. Using this free service, authors can make their results available to the community, in citable form, before we publish the edited article. This *Accepted Manuscript* will be replaced by the edited, formatted and paginated article as soon as this is available.

You can find more information about *Accepted Manuscripts* in the [Information for Authors](#).

Please note that technical editing may introduce minor changes to the text and/or graphics, which may alter content. The journal's standard [Terms & Conditions](#) and the [Ethical guidelines](#) still apply. In no event shall the Royal Society of Chemistry be held responsible for any errors or omissions in this *Accepted Manuscript* or any consequences arising from the use of any information it contains.

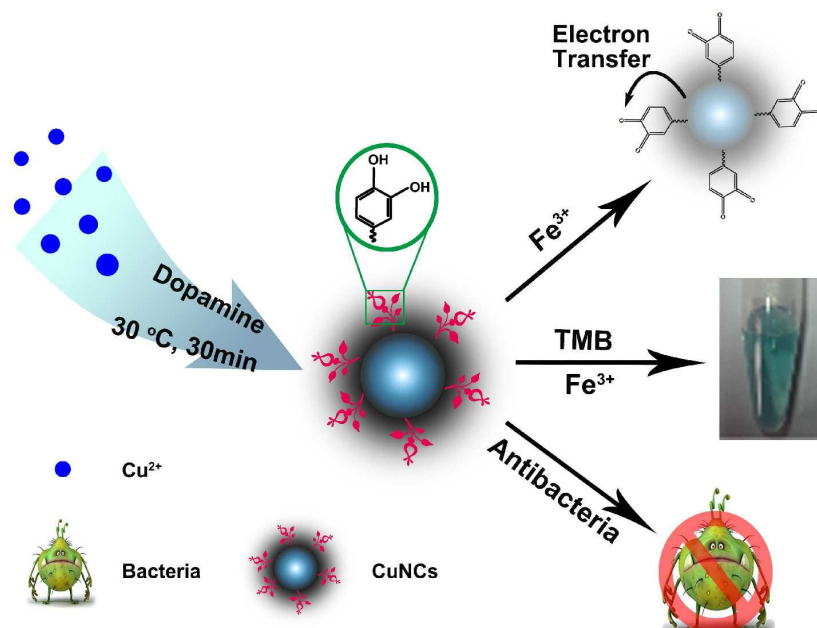
Graphical abstract

for

Dopamine-Derived Copper Nanocrystals as an Efficient Sensing, Catalysis and Antibacterial AgentHong Yan Zou,^{ab} Jing Lan^a and Cheng Zhi Huang *^{ab}

^a Key Laboratory of Luminescence and Real-Time Analytical Chemistry (Southwest University), Ministry of Education, College of Pharmaceutical Sciences, Southwest University, Chongqing, 400715, P. R. China, E-mail: chengzhi@swu.edu.cn, Tel: (+86) 23 68254659, Fax: (+86) 23 68367257.

^b College of Chemistry and Chemical Engineering, Southwest University, Chongqing, 400715, P. R. China.



This study innovatively developed an effective method to synthesize highly luminescent dopamine-derived copper nanocrystals (CuNCs) showing multifunctional properties.



Dopamine-Derived Copper Nanocrystals as an Efficient Sensing, Catalysis and Antibacterial Agent

Hong Yan Zou,^{ab} Jing Lan^a and Cheng Zhi Huang^{* ab}

Received 00th January 20xx,
Accepted 00th January 20xx

DOI: 10.1039/x0xx00000x

www.rsc.org/

A simple one-pot synthesis method for small copper nanocrystals (CuNCs) was developed by employing dopamine (DA) as a reducing and capping reagent. The as-prepared CuNCs exhibited a fluorescence emission at 390 nm, good peroxidase-mimic catalytic property, and excellent antibacterial activities against gram-positive *Staphylococcus aureus* (*S. aureus*). Based on the fluorescence and peroxidase-mimic catalytic features, sensing for Fe³⁺ was made since Fe³⁺ ions have specific interactions with the catechol groups on the surface of CuNCs with the limits of detection of 1.2 μM and 4.2 μM, respectively, which were much lower than the maximum level (5.4 μM) of Fe³⁺ permitted in drinking water by the U.S. Environmental Protection Agency. As for the antibacterial activities, a minimum inhibitory concentration (MIC) of 158 μg mL⁻¹ were found due to the generation of reactive oxygen species (ROS).

Introduction

The ultrasmall nanocrystals bridge the size scales of molecular species and larger nanoparticles or microparticles. They usually reveal fancy properties, such as size-dependent fluorescence, high surface energy, and antibacterial activity, which makes them promising candidates in the fields of sensing, catalytic and biological applications.¹⁻⁵ Much work has already been explored for these fluorescent metal nanoparticles such as gold and silver.⁶⁻¹⁰ Meanwhile, reports on the synthesis and properties of fluorescent copper nanocrystals (CuNCs) are emerging due to their low cost and unique optical and catalytic properties.¹¹⁻¹⁵ Compared to the counterparts, however, fluorescent CuNCs have attracted less attention due to the synthetic difficulty in controlling ultrafine size and the susceptibility to oxidation upon exposure to air. Recently, Jia et al. developed a thiolate ligand CuNCs which has the features of aggregation induced fluorescence enhancement.^{16, 17} When they were used for real applications, wherein the selected thiolate ligands, just like the synthesis of Au nanoparticles,¹⁸ must play two roles, one is to regulate the CuNCs emissions, and the other to molecularly recognize target species. The thiolate ligand CuNCs are interesting but it has the difficulty to

find dual-functional thiolate ligands. So, developing effective method to synthesize brightly luminescent and stable CuNCs with a straight and the specific interactions between target species is highly desirable, which, if realized, would open up possibilities of an array of their practical application.

Dopamine, a famous hormone and neurotransmitter of the catecholamine and phenethylamine families, has received attention for it can act as biocompatible surface stabilizing ligand and reducing agent.^{19, 20} Furthermore, the most interesting properties of dopamine is that it can form versatile biopolymers with many active functional groups such as amines and catechols, which can further interact with other substrates. Recently, dopamine has been used as reducing agent to synthesis copper nanoparticles.²¹ However, the use of dopamine as capping/reducing reagent for the synthesis of luminescent CuNCs has not been reported.

Meanwhile, copper species are known to exhibit antibacterial activity against a wide variety of bacterial strains.²² Esteban-Cubillo *et al.* have demonstrated bactericidal properties of Cu nanoparticles prepared in the matrix of sepiolite.²³ And Mallick *et al.* reported the good antimicrobial activity for the iodine-stabilized Cu Nanoparticle with chitosan.²⁴ However, the mechanism behind this phenomenon still remains debatable. So it is important to study the antimicrobial activities of prepared CuNCs and address the issue of the species involved in the mechanism of action.

To achieve the above goals, remarkable progress has been made to prepare Cu nanomaterials by different chemical modification and asking functional capping reagent with unique and tunable properties for help.²⁵⁻³² However, reduced sensitivity by specific interactions between target

^a Key Laboratory of Luminescence and Real-Time Analytical Chemistry (Southwest University), Ministry of Education, College of Pharmaceutical Sciences, Southwest University, Chongqing, 400715, P. R. China, E-mail: chengzhi@swu.edu.cn, Tel: (+86) 23 68254659, Fax: (+86) 23 68367257.

^b College of Chemistry and Chemical Engineering, Southwest University, Chongqing, 400715, P. R. China.

Electronic Supplementary Information (ESI) available: experiment details, characterization, and some optimization see DOI: 10.1039/x0xx00000x

species limit their pervasive and multi-application. So, there is still plenty of room for improving the performances of Cu nanoparticles. Herein, we proposed a one-pot synthesis strategy to prepare small dopamine-derived multifunctional CuNCs. The CuNCs prepared displayed several advantages over the Cu nanoparticles²¹ reported. First, They showed bright fluorescence and good peroxidase-mimic catalytic property. Second, By taking advantage of the capping agent, specific interactions between catechol groups of dopamine on the surface of CuNCs and Fe³⁺ ions, dual sensing models (the fluorescent and catalytic based sensing system) were applied for the sensitive and selective detection of Fe³⁺ ions. What was more, the CuNCs showed good antibacterial ability, allowing effective killing of *S. aureus* under a low concentration. And the mechanism of the antibacterial ability of CuNCs was investigated. Thus, our study presented a multifunctional nanomaterial as an efficient agent for sensing, catalysis and antibacterial applications.

Experimental Section

Chemicals and materials

Copper sulfate (CuSO₄·5H₂O, 99%) was purchased from Sinopharm Chemical Reagent Co., Ltd. (Shanghai, China). Dopamine hydrochloride (DA) and dichlorodihydrofluorescein diacetate (DCFH-DA) were purchased from Sigma-Aldrich (Steinheim, Germany). Standard stock solutions of Fe³⁺ ion were prepared with FeCl₃ in deionized water. Different concentrations of Fe³⁺ ion were obtained by diluting standard stock solutions. All other reagents were of analytical reagent grade and used as received. All experiments were carried out in aqueous BR buffer (0.2 M, pH 4.0) unless stated otherwise. Deionized water (18.2 MW; Millipore Co., USA) was used. Other metal salts used in this work included NaCl, KCl, AgNO₃, MgSO₄, CaCl₂, ZnCl₂, CdCl₂, NiCl₂, CoCl₂, HgCl₂, FeCl₂, CuCl₂, Pb(NO₃)₂, and Cr(NO₃)₃.

Apparatus

Transmission electron microscopy (TEM) measurements and Energy-dispersive X-ray spectroscopy (EDS) were obtained from a Tecnai G2 F20 S-TWIN microscope (FEI, USA). Atomic force microscopy (AFM) images were captured on a Dimension Icon Scan Asyst atomic force microscope (Bruker Co.). The X-ray photoelectron spectroscopy (XPS) analysis was conducted by an ESCALAB 250 X-ray photoelectron spectrometer (Thermo, USA). The samples for XPS were made by the deposition of a nanocrystal suspension in water on Si substrate. A Fourier transform infrared (FT-IR) spectrophotometer (FTIR-8400S, Shimadzu, Japan) was employed to measuring the FT-IR spectrum. Hydrodynamic diameter and Zeta potential of CuNCs were measured by dynamic light scattering (DLS) and electrophoretic light scattering (ELS) (ZEN3600, Malvern). UV-vis-NIR absorption spectra were obtained using a Hitachi U-3600 spectrophotometer. Steady-state fluorescence spectra were measured with an F-2500 fluorescence spectrophotometer (Hitachi, Japan) with the nanoparticles dispersed in reagents. Fluorescence lifetimes were measured by an FL-TCSPC fluorescence spectrophotometer (Horiba Jobin Yvon Inc., France) using a NanoLED laser light source at the respective

excitation wavelength of the dyes. The data were fitted by a double-exponential decay model.

Preparation of CuNCs

The ultras-small copper nanocrystals were prepared by combining aqueous CuSO₄·5H₂O (Shanghai, China) with dopamine hydrochloride solution. A typical preparation was composed of 1 mL CuSO₄ (0.1 M), 1 mL dopamine hydrochloride (DA, 0.1 M), and 3 mL deionized water by volume (DA: Cu²⁺=1). The solutions were combined, mixed well, and allowed to react with constant magnetic stirring at 30 °C. The solution became yellow over the course of 30 min of reaction under ambient temperature. Then it was purified through a 10 kDa dialysis membrane for 24 hours with distilled water.

Fluorescence Detection of Fe³⁺ ions

The detection of Fe³⁺ ion was performed in BR buffer (0.2 M, pH 4.0). In a typical assay, CuNCs (100 μL, 870 μg mL⁻¹) dispersion was added into BR buffer (200 μL, pH 4.0), followed by the addition of different concentrations of Fe³⁺ ion (0, 5, 10, 20, 40, 80, 100, 150, 200, 300, 400, 500, 600, 700, 800, 1000 μM) and water to 500 μL. The FL spectra were recorded after reaction for 30 min. The selectivity for Fe³⁺ was confirmed by adding other metal ion stock solutions (Na⁺, K⁺, Ag⁺, Mg²⁺, Ca²⁺, Zn²⁺, Cd²⁺, Ni²⁺, Co²⁺, Hg²⁺, Fe²⁺, Cu²⁺, Pb²⁺, Cr³⁺) instead of Fe³⁺ in a similar way.

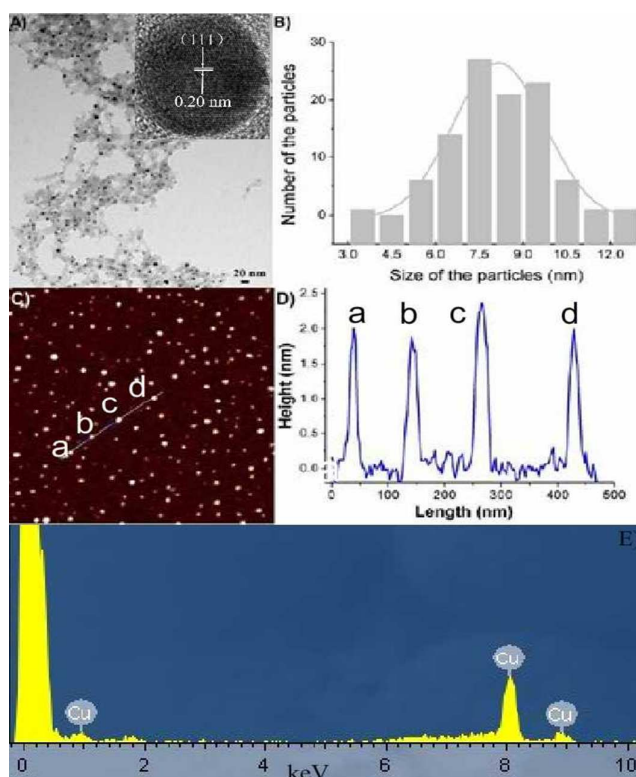


Figure 1. Structure characterization of CuNCs. (A) TEM image of the small CuNCs (inset: high-resolution TEM image). (B) Size

distributions of the small CuNCs obtained by counting 100 particles. (C) AFM image of the small CuNCs. (D) The height of the CuNCs along the line in panel (C). (E) EDS of the particles shown in panel (A).

Peroxidase-mimic based detection of Fe³⁺ ions

The detection of Fe³⁺ ion was performed in BR buffer (0.2 M, pH 4.0) solution. In a typical assay, CuNCs (100 μ L, 870 μ g mL⁻¹) and TMB (100 μ L, 1 mM) dispersion were added into BR buffer (200 μ L, pH 4.0), followed by the addition of different concentrations of Fe³⁺ ion (0, 6, 10, 16, 20, 25, 30, 40, 50, 80, 100, 160, 200 μ M) and water to 500 μ L. The UV-vis spectra (652 nm) were recorded after reaction for 30 min. The selectivity for Fe³⁺ was confirmed by adding other metal ion stock solutions (Na⁺, K⁺, Ag⁺, Mg²⁺, Ca²⁺, Zn²⁺, Cd²⁺, Ni²⁺, Co²⁺, Hg²⁺, Fe²⁺, Cu²⁺, Pb²⁺, Cr³⁺) instead of Fe³⁺ in a similar way. All experiments were performed at room temperature.

In vitro antibacterial activity assay

In this study, *S. aureus* was used as a model bacterium to evaluate the antibacterial activity of the CuNCs adsorbed on the agar surface. For the qualitative analysis, the inhibition zone of the *S. aureus* cultured on Luria-Bertani (LB) agar plates was assessed.³² Briefly, *S. aureus* suspension was first spread on the agar plates, and the test samples (100 μ L) were added on the agar plates. The bacteria were then incubated at 37°C for 24 h, and the inhibition zone was visually inspected for each sample on the plates. The outer and inner diameters and the calculated diameter difference were measured.

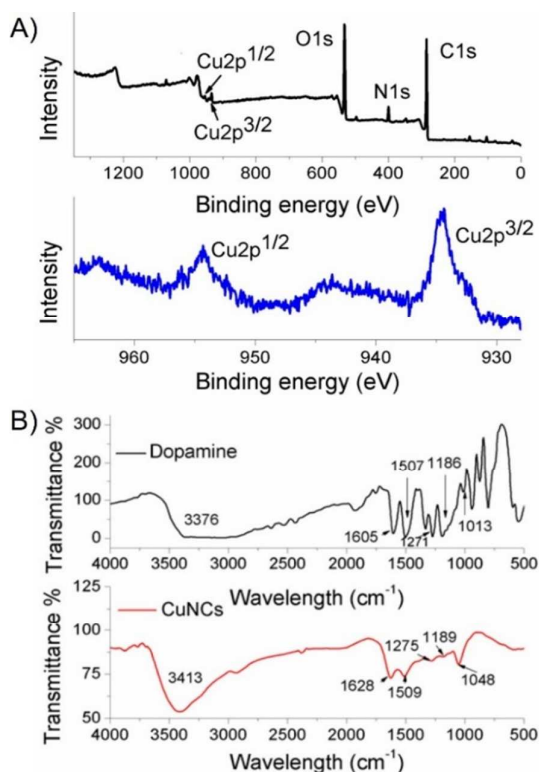


Figure 2. (A) XPS of the CuNCs (upper) and the high-resolution spectra of Cu 2p^{1/2} and Cu 2p^{3/2} (lower); (B) FT-IR spectrum of free dopamine molecule and CuNCs.

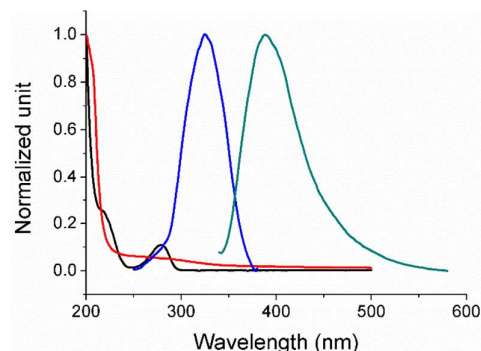


Figure 3. UV-vis absorption of dopamine (black line) and CuNCs (red line); Fluorescence excitation (blue line, emission at 390 nm) and emission (dark cyan line, excitation at 320 nm) spectra of the CuNCs.

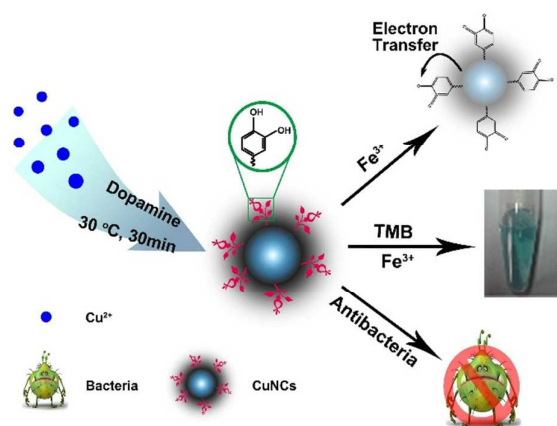
Results and Discussion

Materials characterization

CuNCs were prepared by a one-step convenient synthesis method. The morphology of the CuNCs was characterized using transmission electron microscopy (TEM) and atomic force microscopy (AFM). The TEM image showed that the CuNCs were well dispersed and the average diameter was about 8 nm (Figure 1A, B). High-resolution TEM (HRTEM) analysis was performed to study the nanostructures of CuNCs at the lattice plane level (Figure 1A inset). Fringes with an inter-planar spacing of 0.20 nm were identified, which was attributed to the (111) diffraction plane of face-centered Cu (JCPDS 89-2838). The AFM image (Figure 1C, D) showed that the height of the CuNCs was about 2 nm with a uniform distribution. Peaks of Cu were recorded in Figure 1E, which confirmed the presence of CuNCs by the EDS elemental analysis.

X-ray photoelectron spectroscopy (XPS) analysis (Figure 2A) was carried out to determine the oxidation state of Cu in the samples. An XPS survey spectrum showed that samples were composed of all the expected elements C, O, N, and Cu. Two intense peaks around 951.9 and 932.3 eV were assigned to Cu 2p^{1/2} and 2p^{3/2}, which were attributed to Cu (0) or Cu (I) and consistent with the previous report.³³ Although it was hard to distinguish those from the Cu (I) from Cu (0) due to a very small difference in their binding energy values (about 0.1 eV), the small shoulder near 942 eV implied the presence of Cu (II) states.¹⁶

FT-IR was used to gain understanding of the functional groups involved in the nanoparticle. Representative spectra of the CuNCs and dopamine were shown in Figure 2B. The general features of CuNCs were common to those of dopamine suggesting that the similar functional groups and structures



were likely responsible for the formation and dopamine capping of nanoparticles prepared. The absorption bands in 900–1300 cm^{-1} attributed to benzene ring and phenol hinted the existence of dopamine. The broad bands observed near 3400 cm^{-1} were likely due to –O–H stretch from hydroxyl groups and stretching Scheme 1. Schematic illustration of the synthesis of dopamine-derived CuNCs and their multifunctional properties. (upper) Schematic illustration of the fluorescence response of the dopamine-derived CuNCs to Fe^{3+} ions. (middle) Schematic representation of peroxidase-mimic catalytic colour reaction of TMB with dopamine-derived CuNCs and Fe^{3+} ions. (lower) Schematic illustration of using dopamine-derived CuNCs for antibacterial application.

vibration of N–H bonds. The 1601 cm^{-1} presented the overlap of C=C resonance vibrations in aromatic ring and 1519 cm^{-1} can be ascribed to N–H scissoring vibrations.^{34,35}

As depicted in Figure 3, absorption spectra with a monotonically exponentially increasing spectrum toward shorter wavelengths, indicated the formation of small CuNCs.³⁶ Upon excitation at 320 nm, the CuNCs in aqueous solution displayed one emission peak at 390 nm. When dissolved in aqueous solution, the quantum yield (QY) of CuNCs was 9.6% (Figure S1) against the reference of quinine sulfate. And the PL lifetime of the emission at 390 nm was 1.03 ns (Figure S2, Table S1), which was in the scope of PL decays of many fluorescent zero-valence metal NCs and attributed to emission from singlet excited states.³⁷ Moreover, the fluorescence intensity of CuNCs clearly varied with the increase of solution pH and the maximal emission can be observed at pH 4 (Figure S3). This pH-dependent PL behavior might result from the pH sensing groups in dopamine on the surface of CuNCs. And the fluorescence intensity of the CuNCs in BR buffer (pH=4) was relatively stable for 24h when it was stocked at room temperature (Figure S4). It can be verified by zeta potential values tested (Figure S5).

Dual sensing models for Fe^{3+} detection

Fe^{3+} are well-known to be high toxic to environment.^{38,39} The detection of such ions is thus highly desired. Fe^{3+} ions can oxidize the catechol groups generating the related quinone

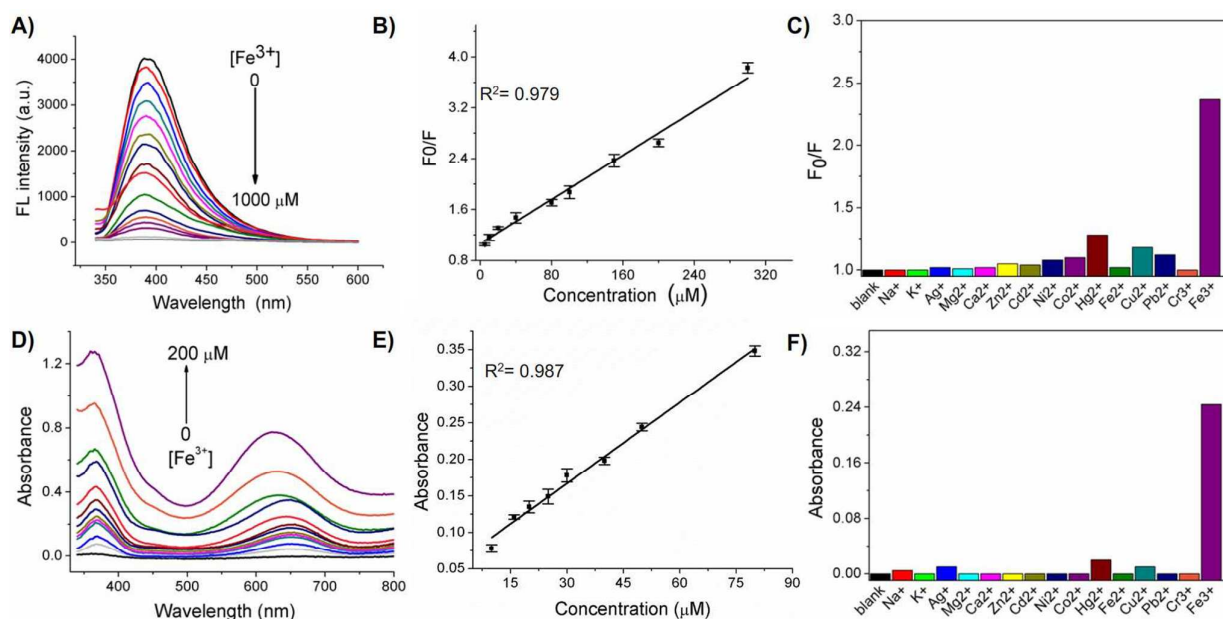


Figure 4. Dual sensing platform for Fe^{3+} detection. (A) Fluorescence spectra of obtained CuNCs ($174 \mu\text{g mL}^{-1}$) in the presence of Fe^{3+} ions with different concentrations (0, 5, 10, 20, 40, 80, 100, 150, 200, 300, 400, 500, 600, 700, 800, 1000 μM). (B) Calibration curve for Fe^{3+} ions detection by fluorescence intensities (F_0/F). (C) Selective relative fluorescent response of CuNCs ($174 \mu\text{g mL}^{-1}$) to specific metal ions (150 μM). (D) UV-vis absorption of the oxidation product of TMB with increasing Fe^{3+} concentrations (0, 6, 10, 16, 20, 25, 30, 40, 50, 80, 100, 160, 200 μM) with CuNCs ($174 \mu\text{g mL}^{-1}$). (E) Calibration curve for Fe^{3+} ions detection by absorbance. (F) Selective relative absorbance response of CuNCs ($174 \mu\text{g mL}^{-1}$) to specific metal ions (150 μM).

absorbance using the peroxidase-like activity of CuNCs. (F) The absorbance at 652 nm of TMB (0.2 mM) with addition of the specific metal ions (50 μM).

TABLE 1 Results of determination of Fe^{3+} in spiked tap water and lake water samples

	Spiked amount (μM)	Measured amount (Recovery), μM		RSD (%)	
Tap water	10	9.90 (99%) ^a	9.79 (97.9%) ^b	2.8 ^a	5.3 ^b
	40	40.2 (100.5%) ^a	39.5 (98.7%) ^b	1.5 ^a	3.5 ^b
	80	80.8 (101.0%) ^a	82.2 (102.8%) ^b	0.5 ^a	5.6 ^b
Lake water	10	10.2 (102.0%) ^a	10.8 (108%) ^b	2.5 ^a	5.8 ^b
	40	40.8 (102.0%) ^a	40.8 (104.5%) ^b	1.0 ^a	3.3 ^b
	80	82.1 (102.6%) ^a	82.8 (103.5%) ^b	1.3 ^a	6.0 ^b

^a determination of Fe^{3+} by the fluorescent sensing and ^b determination of Fe^{3+} by the catalytic based sensing system

molecule (scheme S1), which is a known potent electron-acceptor in biological and abiotic format.^{21,22} It can act as an electron-acceptor quenching the FL of the CuNCs to be used for highly specific detection of Fe^{3+} ions (scheme 1, upper).²³ Thus, we investigated the capability of the prepared fluorescent CuNCs reduced by dopamine for Fe^{3+} ions sensing. As shown in Figure 4A-C, it was clear that the fluorescence of probes were gradually quenched by increasing the concentration of Fe^{3+} ions and a linear detection range from 5 μM to 300 μM was obtained by fitting the plots of relative intensity versus concentration, where the limit of detection (LOD, 1.2 μM) at the signal-to-noise ratio of 3 was lower than the maximum level of Fe^{3+} ions (5.4 μM) permitted in drinking water by the US Environmental Protection Agency.⁴⁰ The response of fluorescent CuNCs to Fe^{3+} ions was much higher than that to other metal ions, attributing to the specific coordination interaction between Fe^{3+} ions and catechol groups on the surface of the CuNCs, which implied an excellent selectivity towards Fe^{3+} ions.

The catalytic activity such as enzyme mimetic property of small nanocrystals have become popular for bio-signal amplification, mainly because of their large surface area and high surface energy.^{3,5} The commonly used target detection involves a chromogenic substrate catalysed in the presence of H_2O_2 such as 3,3',5,5'-tetramethylbenzidine (TMB) to form the coloured product. In the following, the enzyme mimic activity of CuNCs was evaluated in the catalysis of the peroxidase substrate TMB (scheme 1, middle). The CuNCs could catalyze the oxidation of TMB (ox-TMB) in the presence of H_2O_2 and produced a deep blue color, with maximum absorbance at 652 nm. In contrast, CuNCs or H_2O_2 alone did not produce the significant color change (Figure S6). These results confirmed that the CuNCs exhibited peroxidase mimic activity toward TMB with H_2O_2 . As Fe^{3+} ions can oxidize the catechol groups to produce the H_2O_2 (scheme S1),^{21,22} As

shown in Figure 4D-F, the absorbance at 652 nm of TMB was increased by increasing the concentration of Fe^{3+} ions to the CuNCs and TMB solution with a gradient blue color which can be seen by naked eyes (Figure S7). A linear detection range from 10 μM to 80 μM was obtained by fitting the plots of relative intensity versus concentration (LOD=4.2 μM). The selectivity toward Fe^{3+} was also investigated in the presence of other metal ions, as shown in Figure 5C. it was clear that only Fe^{3+} ions resulted in a significant absorbance enhancement (652 nm) of ox-TMB.

To test its practicality, we applied the proposed method to the analysis of the aqueous samples spiked with Fe^{3+} ions (Table 1). The standard addition method was employed to eliminate any matrix effects for synthetic samples prepared with tap water and lake water. The low relative standard deviations (RSDs), ranging from 0.5% to 6.0%, confirmed the accuracy of the two sensing models; thus, the CuNCs probes met the test requirements for environmental analysis.

Antibacterial Property of CuNCs

Moreover, the antimicrobial activity of CuNCs using gram-positive *S. aureus* bacterial strains was studied (Scheme 1C). Clear bacterial inhibition rings were observed showing their good antimicrobial activity depending on the concentration and the MIC was found to be about 158 $\mu\text{g mL}^{-1}$ (Figure 5A, B). In order to study the mechanism of the antimicrobial activity of CuNCs, separate experiments were carried out to evaluate the effect of the reagents involved. As shown in Figure 5C, no antimicrobial activity was detected for the control solution of CuSO_4 and dopamine, which can confirm that the Cu^{2+} is not the main factor for the antimicrobial activity. And the positive charge of CuNCs (20.3 mV) excluded the charge effect. These phenomenon may attribute to some species involved in the mechanism of action.^{41,42} The CuNCs have been reported to produce ROS for the CuNCs with surface modification which can be determined via oxidation of

dichlorodihydrofluorescein (DCFH). The equivalent $[H_2O_2]$ generated by the CuNCs can be calculated and increased with the content of CuNCs (Figure S8, 9). As only the $[H_2O_2]$ generated (9.86 mM) by $791 \mu\text{g mL}^{-1}$ showed no *S. aureus* growth inhibition too, the antibacterial activity of the CuNCs may attribute to the interactions between nanoparticles and the ROS generated. When the oxygen was adsorbed at the surface of nanoparticles, resulting in a contact potential difference between metal and adsorbed oxygen, A Fenton-like process could occur with

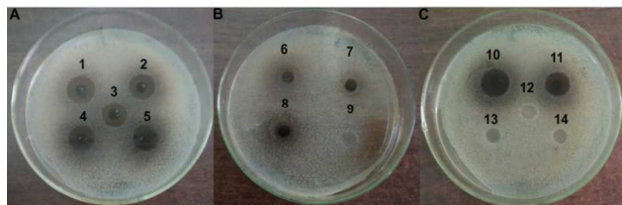


Figure 5. Growth inhibition of *S. aureus* bacteria on agar plate for different samples. (A, B) The antimicrobial activity shown with the decreasing concentration of CuNCs. Spots 1-9 represent $791, 712, 633, 554, 475, 475, 317, 158, 79 \mu\text{g mL}^{-1}$ of the CuNCs. (C) Separate experiments for evaluating the antimicrobial activity with $792 \mu\text{g mL}^{-1}$ CuNCs (spot 10), $554 \mu\text{g mL}^{-1}$ CuNCs (spot 11), $9.86 \text{ mM H}_2\text{O}_2$ (spot 12), 0.02 M CuSO_4 (spot 13), 0.02 M dopamine (spot 14).

copper ions ($\text{Cu(I)} + \text{H}_2\text{O}_2 \rightarrow \text{Cu(II)} + \text{OH}^- + \text{HO}^\cdot$) accordance to the XPS of the Cu (II) releasing.⁴³ Additional studies are needed to determine the role of ROS in antibacterial activity of CuNCs because of the complexity in biological environments.

To confirm the proposed CuNCs with good multifunctional property, we carry out a literature review of the Cu clusters or nanoparticles used as sensing, catalysis and antibacterial reagent (TableS2-4). As can be observed, most of the given examples shown only one or two types of properties which does not take into account factors, such as specific interactions with target, and special species involved in the mechanism of action. To further confirm and optimize the good performance of the CuNCs prepared, selectivity experiments were carried out using different CuNCs synthesized by various molar ratio of DA to copper salt (1:3, 1:2, 1:1, 2:1, 3:1) (Figure S10-16). It can be seen that the CuNCs synthesized (DA: Cu^{2+} =1:1) showed best sensing ability for Fe^{3+} detection. And all the CuNCs showed good antimicrobial activity. which further supported the the synthesized CuNCs are quite promising in analytical and biological applications.

Conclusions

In summary, we presented a facile method for the preparation of highly luminescent and peroxidase-mimic CuNCs. with the dopamine as the reducing and capping reagent. By taking advantage of the specific interactions between catechol groups on the surface of CuNCs and Fe^{3+} ions, dual sensing models (the fluorescence and peroxidase-mimic based sensing system) were applied for the sensitive and selective detection of Fe^{3+} ions. The antibacterial activity of CuNCs showed a

distinctive concentration dependence. And this enhancement effect may be attributed to the ROS generated by the CuNCs after surface modification with dopamine. In view of the convenient synthesis route and attractive multifunctional properties, the synthesized CuNCs are quite promising in diverse analytical and biological applications. Further studies are needed to determine the role of ROS in antibacterial activity of CuNCs because of the complexity in biological environments.

Acknowledgements

This study was financially supported by the National Natural Science Foundation of China (NSFC, Grant No. 21375109) and Chongqing Postdoctoral Science Foundation funded project (Xm2014021).

Notes and references

1. Y. Lu, and W. Chen, *Chem. Soc. Rev.*, 2012, **41**, 3594–3623.
2. H. Qian, M. Zhu, Z. Wu and R. Jin, *Acc. Chem. Res.*, 2012, **45**, 1470–1479.
3. J. J. Li, J. J. Zhu and K. Xu, *TrAC-Trends Anal. Chem.*, 2014, **58**, 90–98.
4. O. V. Kharisova, B. I. Kharisov, V. Manuel Jimenez-Perez, B. Munoz Flores and U. Ortiz Mendez, *RSC Adv.*, 2013, **3**, 22648–22682.
5. Y. H. Lin, J. S. Ren and X. G. Qu, *Adv. Mater.*, 2014, **26**, 4200–4217.
6. A. Leifert, Y. Pan-Bartnek, U. Simon and W. Jahnen-Dechent, *Nanoscale*, 2013, **5**, 6224–6242.
7. K. Huang, H. Ma, J. Liu, S. Huo, A. Kumar, T. Wei, X. Zhang, S. Jin, Y. Gan, P. C. Wang, S. He, X. Zhang, and X. Liang, *ACS Nano*, 2012, **6**, 4483–4493.
8. D. W. Guo, L. Y. Zhu, Z. H. Huang, H. X. Zhou, Y. Ge, W. J. Ma, J. Wu, X. Y. Zhang, X. F. Zhou, Y. Zhang, Y. Zhao and N. Gu, *Biomaterials*, 2013, **34**, 7884–7894.
9. J. Lan, P. Zhang, T. T. Wang, Y. Chang, S. Q. Lie, Z. L. Wu, Z. D. Liu, Y. F. Li and C. Z. Huang, *Analyst*, 2014, **139**, 3441–3445.
10. K. Zhang, K. Wang, X. Zhu, J. Zhang, L. Xu, B. Huang and M. H. Xie, *Chem. Commun.*, 2014, **50**, 180–182.
11. X. F. Jia, J. Li, L. Han, J.T. Ren, X. Yang and E. Wang, *ACS Nano*, 2012, **6**, 3311–3317.
12. L. I. Zhang, J. J. Zhao, M. Duan, H. Zhang, J. H. Jiang and R. Q. Yu, *Anal. Chem.*, 2013, **85**, 3797–3801.
13. A. D. Brumbaugh, K. A. Cohen and S. K. S. Angelo, *ACS Sustainable Chem. Eng.*, 2014, **2**, 1933–1939.
14. B.W. Wang, S.X. Chen, J. Nie and X. Q. Zhu, *RSC Adv.*, 2014, **4**, 27381–27388.
15. X. J. Zhao and C. Z. Huang, *New J. Chem.*, 2014, **38**, 3673–3677.
16. X. F. Jia, J. Li, and E. Wang, *Small*, 2013, **9**, 3873–3879.
17. X. F. Jia, X. Yang, J. Li, D. Y. Li, E. Wang, *Chem. Commun.*, 2014, **50**, 237–239.
18. Z. T. Luo, X. Yuan, Y. Yu, Q. B. Zhang, D. T. Leong, J. Y. Lee and J. P. Xie, *J. Am. Chem. Soc.*, 2012, **134**, 16662–16670.
19. H. Lee, S. M. Dellatore, W. M. Miller and P. B. Messersmith, *Science*, 2007, **318**, 426–430.
20. H. Lee and P. B. Messersmith, *Adv. Mater.*, 2009, **21**, 431–434.
21. J. Xiong, X. D. Wu and Q. J. Xue, *J. Colloid Interface Sci.*, 2013, **390**, 41–46.
22. N. Cioffi, L. Torsi, N. Ditaranto, G. Tantillo, L. Ghibelli, L. Sabbatini, T. Bleve-Zacheo, M. D'Alessio, P. Giorgio Zamboni and E. Traversa, *Chem. Mater.*, 2005, **17**, 5255–5262.
23. A. Esteban-Cubillo, C. Pecharrroman, E. Aguilar, J. Santaren and

- J. S. Moya, *J. Mater. Sci.*, 2006, **41**, 5208–5212.
24. S. Mallick, S. Sharma, M. Banerjee, S. S. Ghosh, A. Chattopadhyay and A. Paul, *ACS Appl. Mater. Interfaces*, 2012, **4**, 1313–1323.
25. H. Y. Cao, Z. H. Chen, H. Z. Zheng and Y. M. Huang, *Biosen. Bioelectron.*, 2014, **62**, 189–195.
26. N. Goswami, A. Giri, M. S. Bootharaju, P. Lourdu Xavier, T. Pradeep and S. Kumar Pal, *Anal. Chem.*, 2011, **83**, 9676–9680.
27. N. Vilar-Vidal, J. Rivas and M. A. López-Quintela, *ACS Catal.*, 2012, **2**, 1693–1697.
28. N. Vilar-Vidal, J. Rivas and M. A. López-Quintela, *Small*, 2014, **10**, 3632–3636.
29. L. Hu, Y. Yuan, L. Zhang, J. Zhao, S. Majeed, and G. Xu, *Anal. Chim. Acta.*, 2013, **762**, 83–86.
30. L. Rastogi and J. Arunachalam, *Colloid Surf. B-Biointerfaces*, 2013, **108**, 134–141.
31. B. J. Li, Y. Y. Li, Y. H. Wu and Y. B. Zhao, *Mater. Sci. Eng. C*, 2014, **35**, 205–211.
32. V. J. Boyle, M. E. Fancher and R. W. Ross, *Antimicrob. Agents and Ch.*, 1973, **3**, 418–424.
33. S. Q. Lie, D. M. Wang, M. X. Gao, and C. Z. Huang, *Nanoscale*, 2014, **6**, 10289–10296.
34. R. F. Luo, L. L. Tang, S. Zhong, Z. L. Yang, J. Wang, Y. J. Weng, Q. F. Tu, C. X. Jiang and N. Huang, *ACS Appl. Mater. Interfaces*, 2013, **5**, 1704–1714.
35. S. Hong, Y. S. Na, S. Choi, I. T. Song, W. Y. Kim and H. Lee, *Adv. Funct. Mater.*, 2012, **22**, 4711–4717.
36. A. D. Brumbaugh, K. A. Cohen and S. S. Angelo, *ACS Sustainable Chem. Eng.*, 2014, **2**, 1933–1939.
37. J. Zheng, C. Zhang and R. M. Dickson, *Phys. Rev. Lett.*, 2004, **93**, 077402.
38. S. W. Zhang, J. X. Li, M. Y. Zeng, J. Z. Xu, X. K. Wang and W. P. Hu, *Nanoscale*, 2014, **6**, 4157–4162.
39. B. Xiong, Y. Chen, Y. W. Shu, B. Shen, H. N. Chan, Y. Z. Chen, J. L. Zhou and K. K. Wu, *Chem. Commun.*, 2014, **50**, 13578–13580.
40. S. Mirlohi, A. M. Dietrich and S. E. Duncan, *Environ. Sci. Technol.*, 2011, **45**, 6575–6583.
41. M. Shi, H. S. Kwon, Z. M. Peng, A. Elder and H. Yang, *ACS Nano*, 2012, **6**, 2157–2164.
42. C. Chen, I. Ahmed and L. Fruk, *Nanoscale*, 2013, **5**, 11610–11614.
43. L. Macomber, C. Rensing and J. A. Imlay, *J. Bacteriol.*, 2007, **189**, 1616–1626.